sessions, participants completed a range of tasks, including high- and low-*g* spatial (Fig. 1A); high- and low-*g* verbal (Fig. 1B); and two standard measures of *g*, Cattell's Culture Fair, Scale 2 Form B (*17*) (mean score in our sample 34/46 items correct, range 24 to 43), and the verbal scale of the AH4 (*18*) (mean score in our sample 43/65 items correct, range 27 to 58). To obtain an overall measure of *g* for each participant, scores on the latter pair of tasks were standardized and averaged. Further data on the two verbal tasks, again completed with a range of other tasks, were obtained in a second study of 46 participants, mean age 42 (range 35 to 51). In this study, the measure of *g* was Cattell's Culture Fair, Scale 2 Form A, with one section omitted because of overlap with other tasks in the study (mean score in our sample 24/34 items correct, range 12 to 31). For the spatial and verbal tasks, overall mean scores (number correct in 4 min) were as follows: high-*g* spatial, 12 (range 4 to 18); low-*g* spatial, 198 (range 162 to 225); high-*g* verbal, 7 (range 1 to 17); low-*g* verbal, 41 (range 16 to 75).

10. PET was used to obtain regional cerebral bloodflow (rCBF) data in 13 right-handed participants, mean age 26 (range 21 to 34). PET imaging was approved by the Ethics Committee of Heinrich-Heine-University Düsseldorf (Application 868). Measurements were made with an eight-ring PET camera (PC4096 plus, GE/Scanditronix, Uppsala, Sweden). The session included six scans (one for each of the tasks described in this report, plus one more of no relevance here), with the order of tasks approximately counterbalanced across participants. To allow for decay of radiation (*19*), successive scans were separated by 15 min, toward the end of which the 0.5-min practice period (see legend to Fig. 1) of the next task was given. For each scan, 1480 MBq of [^{15}O]butanol was injected into the right brachial vein, flushed with 10 ml of saline. PET scanning and the 2-min task period (see legend to Fig. 1) began at the moment of the injection, so that the participant was fully engaged in the task when radioactivity reached the brain about 11 s later. As previously described (*20*), rCBF was calculated from the first 40 s of dynamically recorded head uptake data.
11. PET image slices were reconstructed with a Hanning filter to an effective image resolution (full width at half maximum, FWHM) of 9 mm with a slice thickness of 6.4 mm. Further analysis was undertaken with SPM99 (www.fil.ion.ucl.ac.uk/spm). Scans for each subject were realigned, spatially normalized onto the PET template, and smoothed with an isotropic Gaussian kernel with FWHM set at 16 mm. The SPM99 gray matter threshold was set to its default value. For task comparisons, an ANCOVA (analysis of covariance) model was fitted to the data for each voxel. To remove confounds due to head movement across scans (*21*), we tested *F*-value images to determine whether scan order or any of the six head movement parameters were significantly associated with rCBF values (*22*). Those parameters with significant associations (scan order, translation in z, rotation in *x*) were set as covariates of no interest, along with global blood flow. In this report we describe only relative increases in rCBF (activations) in high-*g* tasks. For the spatial contrast only, there were also significant deactivations (high-*g* < low-*g*) in regions of motor and medial premotor cortex, reflecting the higher response rate in the low-*g* task, and bilaterally at the temporoparietal junction.
12. M. Corbetta, F. M. Miezin, G. L. Shulman, S. E. Petersen, *J. Neurosci.* **13**, 1202 (1993); S. M. Courtney, L. Petit, J. Ma. Maisog, L. G. Ungerleider, J. V. Haxby, *Science* **279**, 1347 (1998); E. Wojciulik and N. Kanwisher, *Neuron* **23**, 747 (1999).
13. G. Esposito, B. S. Kirkby, J. D. Van Horn, T. M. Ellmore, K. F. Berman, *Brain* **122**, 963 (1999); V. Prabhakaran, J. A. L. Smith, J. E. Desmond, G. H. Glover, J. D. E. Gabrieli, *Cogn. Psychol.* **33**, 43 (1997).
14. Mean values of estimated global blood flow (ml dl^{-1} min^{-1}) for each task were as follows: high-*g* spatial, 49.4; low-*g* spatial, 49.9; high-*g* verbal, 49.8; low-*g* verbal, 49.7.
15. The circles task was included in the first behavioral study (*9*) and the PET session (*10*). In the behavioral study, mean score (number correct in 4 min) was 87 (range 53 to 112). In PET, the mean estimated global blood flow (ml dl^{-1} min^{-1}) was 49.4.
16. J. Duncan and A. M. Owen, *Trends Neurosci.*, in press.
17. Institute for Personality and Ability Testing, *Measuring Intelligence with the Culture Fair Tests* (The Institute for Personality and Ability Testing, Champaign, IL, 1973).
18. A. W. Heim, *AH4: Group Test of General Intelligence* (NFER-Nelson, Windsor, UK, 1970).
19. H. Herzog *et al.*, *Eur. J. Nucl. Med.* **21**, 138 (1994).
20. H. Herzog, R. J. Seitz, L. Tellmann, H.-W. Müller-Gärtner, *J. Cereb. Bloodflow Metab.* **16**, 645 (1996).
21. M. Brett, P. Bloomfield, D. J. Brooks, J. F. Stein, P. M. Grasby, *Neuroimage* **9**, S56 (1999).
22. K. J. Worsley, J.-B. Poline, K. J. Friston, A. C. Evans, *Neuroimage* **6**, 305 (1997).
23. J. Talairach and P. Tournoux, *Co-Planar Stereotaxic Atlas of the Human Brain* (Thieme, New York, 1988).
24. R. B. Ekstrom, J. W. French, H. H. Harmon, D. Derman, *ETS Kit of Factor-Referenced Cognitive Tests* (Educational Testing Service, Princeton, NJ, 1976).
25. W. Wothke *et al.*, *Rep. No. AFHRL-TR-90-67* (Air Force Human Resources Laboratory, Brooks Air Force Base, TX, 1991).

10 March 2000; accepted 26 May 2000

The Role of GTP-Binding Protein Activity in Fast Central Synaptic Transmission

Tomoyuki Takahashi,* Tetsuya Hori, Yoshinao Kajikawa, Tetsuhiro Tsujimoto

Guanosine 5′-triphosphate (GTP)–binding proteins (G proteins) are involved in exocytosis, endocytosis, and recycling of vesicles in yeast and mammalian secretory cells. However, little is known about their contribution to fast synaptic transmission. We loaded guanine nucleotide analogs directly into a giant nerve terminal in rat brainstem slices. Inhibition of G-protein activity had no effect on basal synaptic transmission, but augmented synaptic depression and significantly slowed recovery from depression. A nonhydrolyzable GTP analog blocked recovery of transmission from activity-dependent depression. Neither effect was accompanied by a change in presynaptic calcium currents. Thus, G proteins contribute to fast synaptic transmission by refilling synaptic vesicles depleted after massive exocytosis.

Fast synaptic transmission is mediated by quantal packets of neurotransmitters released from synaptic vesicles through exocytosis (*1*). When the synaptic vesicles in the readily releasable pool (RRP) are depleted, they are replenished through vesicle recycling from a reserve pool (*2*). In yeast and mammalian secretory cells, a variety of G proteins are involved in vesicle endocytosis, trafficking, and exocytosis (*3*). However, the functional role of G proteins in fast synaptic transmission remains unclear. Synaptic transmission can be blocked by guanine nucleotide analogs (*4*) or Rab3A-binding peptides (*5*) injected into squid giant nerve terminals, suggesting that monomeric G proteins such as Rab3A may contribute to exocytosis (*4*, *6*). In contrast, exocytosis is inhibited by overexpression of Rab3A or Rab3 regulator proteins in secretory and hippocampal cells, suggesting that this G protein may negatively modulate exocytosis (*7*). As a step toward clarifying the individual roles of G proteins, we studied the overall contribution of presynaptic G-protein activity to fast synaptic transmission by infusing guanine nucleotide analogs into the giant nerve terminal, the calyx of Held, visually identified in slices of rat brainstem (*8*). In this preparation, presynaptic Ca^{2+} currents (I_{pCa}) and glutamatergic excitatory postsynaptic currents (EPSCs) can be recorded simultaneously while drugs of given concentrations are applied into the nerve terminal through a whole-cell pipette (*9*, *10*).

In paired pre- and postsynaptic recordings, EPSCs were evoked stably at 0.1 Hz in a postsynaptic principal cell in the medial nucleus of trapezoid body (MNTB) by presynaptic action potentials elicited at the calyx of Held (*9–11*). Application of guanosine 5′-*O*-(2-thiodiphosphate) (GDPβS, 3 to 6 mM) into the calyx through pipette perfusion blocked G-protein activity, as indicated by a marked reduction of the baclofen-induced EPSC inhibition (*12*), but had no effect on EPSCs (Fig. 1A) (mean amplitude 10 min after infusion = 107 ± 9.8% of control, n = 4). Thus, presynaptic G-protein activity is not immediately required for basal synaptic transmission.

We next examined whether G-protein activity is involved in synaptic depression. EPSCs were evoked by I_{pCa} at 0.1 Hz (*9*, *11*). After a stable epoch, a train of 30 stimuli at 10 Hz depressed EPSC amplitude to 57 ± 7% (mean ± SEM, n = 6), whereas I_{pCa} was not

Department of Neurophysiology, University of Tokyo Faculty of Medicine, Tokyo 113-0033, Japan.

*To whom correspondence should be addressed. E-mail: ttakahas-tky@umin.ac.jp

reduced (*13*), indicating that the synaptic depression was caused by a mechanism downstream of Ca^{2+} influx (Fig. 1B). Because postsynaptic AMPA receptors recover from desensitization within 100 ms (*14*), the depression must be presynaptically mediated, most likely by the depletion of synaptic vesicles in RRP (*15*, *16*), although reduction of release probability (*17*) may be an additional factor. When GTP (0.5 mM) was replaced by GDPβS (3 mM) in the presynaptic pipette, EPSCs were depressed to a greater extent (29 ± 7%; $n = 6$, $P < 0.01$) during the 10-Hz train (Fig. 1, B and C). At lower frequencies (0.2 to 1.0 Hz, 30 stimuli), the effect of GDPβS was not significant (Fig. 1C).

The recovery time from synaptic depression was measured from EPSC amplitude at various time intervals after the 10-Hz train (Fig. 2A). With GTP (0.5 mM) in the presynaptic pipette, the time constant of recovery was 3.32 ± 0.91 s ($n = 7$), whereas with GDPβS, recovery was much slower (time constant, 15.7 ± 2.6 s; $n = 8$, $P < 0.001$) (Fig. 2B). To exclude the possible side effect of GDPβS, we omitted GTP from presynaptic pipettes and washed out endogenous GTP for 20 min after rupture. The recovery time constant then fell to a value between those obtained for GTP and GDPβS (8.44 ± 1.2 s; $n = 9$, significantly different from both, $P < 0.02$) (Fig. 2B). To examine whether this effect is mediated by GTP sites or adenosine triphosphate (ATP) sites through cross talk, we loaded calyces with ATP (10 mM) together with GDPβS (3 mM). The recovery time constant was 13.5 ± 3.4 s ($n = 3$), which was not significantly different from that with GDPβS alone ($P = 0.57$). Thus, G proteins in the nerve terminals play a role in accelerating recovery from synaptic depression.

Both monomeric and heterotrimeric G proteins are potentially involved in accelerating recovery from depression. Mechanisms downstream of heterotrimeric G proteins such as cyclic nucleotide cascades may also be involved. When the intracellular cyclic nucleotide concentration was raised by bath application of forskolin (20 μM) in combination with isobutylmethylxanthine (200 μM), the amplitude of EPSCs increased (by 28 ± 3.6%, $n = 7$). After a 10-Hz train (for 0.3 s), EPSCs recovered with a mean time constant of 3.54 ± 0.30 s, similar to the control value (3.95 ± 0.30 s, $P = 0.42$) [compare with (*15*)]. Thus, cyclic nucleotides do not seem to be involved in recovery after depression.

Next we examined the effect of the nonhydrolyzable GTP analog guanosine 5′-*O*-(2-thiodiphosphate) (GTPγS). When GTPγS (0.2 mM) was infused into the calyx (Fig. 3A), EPSCs gradually diminished concomitantly with I_{pCa} and reached a low, steady level (35 ± 5%, $n = 10$) within 20 min (Fig. 3A) through activation of heterotrimeric G proteins (*9*, *18*). A 10-Hz train administered in the presence of GTPγS (0.2 mM) depressed EPSCs (Fig. 3B) to 46 ± 5%, $n = 9$), a value between those obtained for the control (with GTP) and GDPβS (Fig. 1B). Although I_{pCa} was unchanged throughout, the recovery of EPSCs from depression was incom-

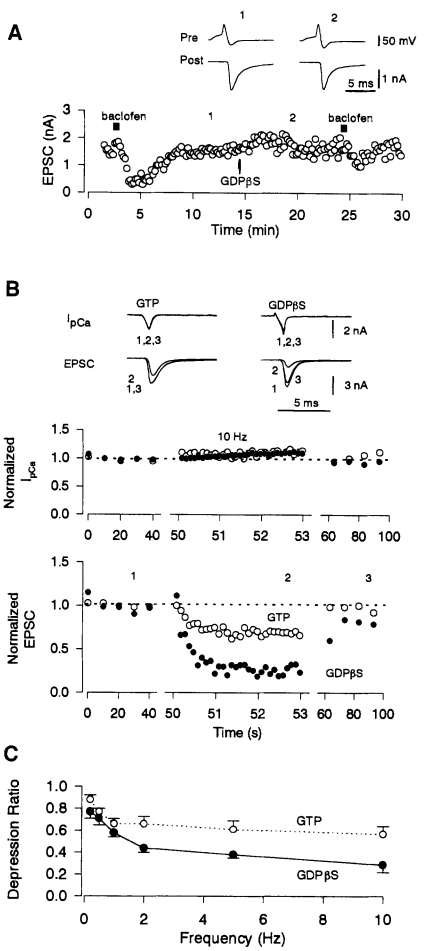

Fig. 1. Effects of GDPβS on basal synaptic transmission and depression. (**A**) EPSCs were evoked by presynaptic action potentials elicited by 1-ms depolarizing current pulse at 0.1 Hz. GDPβS (6 mM) was infused into the calyx (arrow). EPSCs and presynaptic action potentials before (1) and after (2) GDPβS application are shown above the panel. Bath application of baclofen (10 μM, 40 s) (filled bars) was done 10 min before and 10 min after GDPβS application. Sample records were averaged from six consecutive records in this and in subsequent figures. (**B**) EPSCs (lower panel) evoked by I_{pCa} (upper panel) underwent synaptic depression during a train of repetitive stimulation (10 Hz, 3s) and recovered after returning to 0.1 Hz. Synapses with their calyces were loaded either with GDPβS (3 mM) (●) or GTP (0.5 mM) (○). Amplitudes of I_{pCa} and EPSCs are normalized to their mean amplitude at 0.1 Hz before the 10-Hz train. I_{pCa} and EPSCs before (1), during (2), and after (3) the 10-Hz train are superimposed in sample records in the upper panel. (**C**) The frequency dependence of the depression ratio at calyces loaded with GTP (○) or GDPβS (●). Data points and error bars represent the mean ± SEM from five to eight synapses in this and in subsequent figures. The depression ratio was estimated from the mean amplitude of the last five EPSCs during the repetitive stimulation divided by the mean amplitude of five EPSCs in the control at 0.1 Hz. At six synapses, the difference between GTP and GDPβS is significant at 10, 5, and 2 Hz ($P < 0.02$), but insignificant at 1, 0.5, and 0.2 Hz ($P > 0.1$). The mean amplitude of EPSCs (2.43 ± 0.54 nA, $n = 6$) in calyces loaded with GTP is comparable to that with GDPβS (2.04 ± 0.30 nA, $n = 6$).

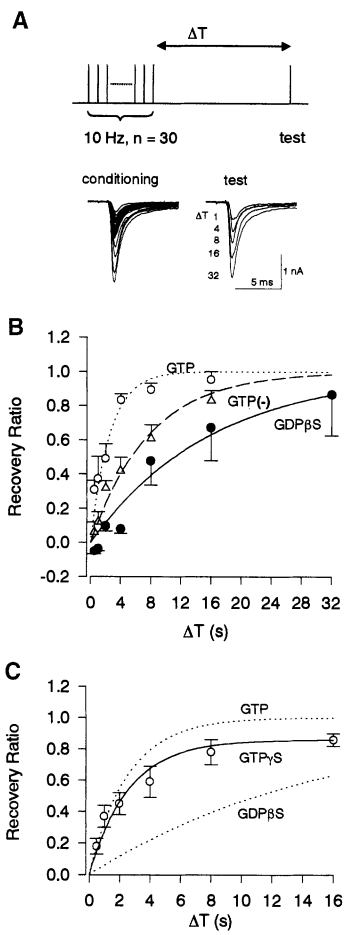

Fig. 2. Effects of guanine nucleotides on the time course of recovery from synaptic depression. (**A**) Experimental protocol and sample recordings of EPSCs during a 10-Hz train (left, superimposed) and of EPSCs evoked by test pulses at different time intervals (ΔT, right, superimposed) after the conditioning train. (**B**) The time course of recovery with GTP ($n = 4$ to 6) (○), with GDPβS ($n = 5$ to 8) (●), or without guanine nucleotides ($n = 8$ to 9, 20 to 40 min after whole-cell recording) (△). Single exponential curves were fit by the least-squares method. The negative values for the first two points (0 and 0.5 s) with GDPβS may be due to the recovery from combined synaptic facilitation masked by depression during high-frequency stimulation. (**C**) Time course of recovery from depression in calyces loaded with GTPγS (0.2 mM, $n = 6$ to 8). The recovery time courses in calyces loaded with GTP or GDPβS are shown by dashed lines.

plete in GTPγS (Fig. 3B) (88 ± 3%, n = 6) (*19*), indicating that the recovery of EPSCs from depression was blocked at the step downstream of Ca^{2+} influx. Despite the incomplete recovery of EPSCs from depression, the rate of recovery was similar to that for the control (GTP, $P >$ 0.6), with a mean time constant of 3.82 ± 0.93 s (n = 7) (Fig. 2C). Thus, GTPγS can replace GTP with respect to the rate but not with respect to the magnitude of recovery.

Tetanic stimulation (100 Hz for 10 s) causes a marked depression of EPSCs accompanied by inactivation of I_{pCa}, which is followed by a gradual recovery owing largely to the recovery of I_{pCa} from inactivation (*20*). In GTPγS, EPSCs no longer recovered from posttetanic depression, whereas I_{pCa} recovered from inactivation with a normal time course (n = 6) (Fig. 4A). EPSCs recovered normally in GDPβS (3 mM) or GTP (0.5 mM) (Fig. 4B). This block of recovery by GTPγS was not associated with a change in quantal size, because the mean amplitude of miniature EPSCs (mEPSCs) was the same after tetanic stimulation (107 ± 8.2%, n = 6) (Fig. 4C). Thus, GTP hydrolysis is essential for EPSCs to recover from synaptic depression (*21*).

Our results indicate that G-protein activity is essential for recovery from synaptic depression. The rate of recovery from depression mainly reflects the rate of RRP replenishment (*15*, *16*), which is accelerated by intracellular Ca^{2+} (*22*). In many cell systems, intracellular Ca^{2+} concentration is affected by inositol phosphates and their receptors, both of which can be up-regulated by heterotrimeric G proteins (*23*). However, at the calyx of Held, loading of inositol 1,4,5-trisphosphate (30 μM) into the nerve terminal had no effect on the EPSC amplitude or the frequency of mEPSCs (*24*). The most plausible candidates for accelerating vesicle replenishment are monomeric G proteins such as Rab or ARF (*3*, *25*), although tyrosine kinase activation by heterotrimeric G proteins (*26*) remains a possibility.

G-protein turnover through GTP hydrolysis is essential for vesicular trafficking in secretory cells (*3*). In isolated nerve-terminal preparations, GTPγS blocks the dynamin-dependent fission process of budded coated vesicles in endocytosis (*27*). In the present study, GTPγS irreversibly diminished EPSCs in an activity-dependent manner without affecting I_{pCa}, recovery rate from depression, or quantal size. GTPγS may block the turnover of dynamin or other G proteins involved in trafficking, thereby possibly immobilizing vesicle recycling. It may then reduce the number of synaptic vesicles at the release site or the available number of release sites.

At the calyx-MNTB synapse, GDPβS had no effect on basal synaptic transmission, and GTPγS attenuated EPSCs only through I_{pCa} suppression. These results cannot be reconciled with the hypotheses that presynaptic G proteins directly modulate the exocytotic process, either positively or negatively (*4*, *6*, *7*), although a possible cancellation of opposite effects in blocking overall G-protein activity cannot be excluded from our present study. It is also possible that the role of G proteins differs among cell types and species.

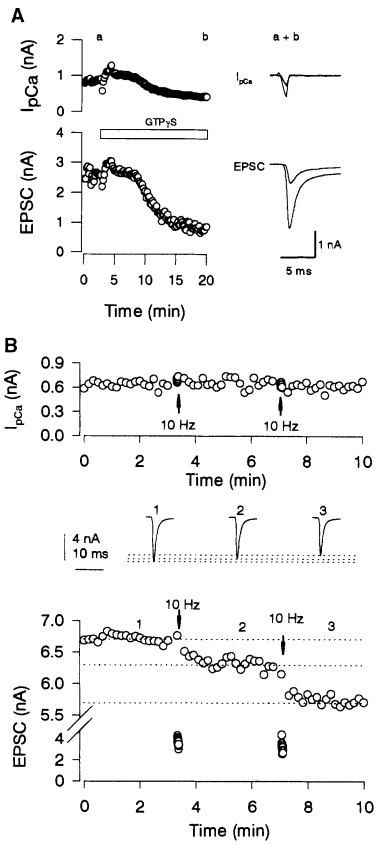

Fig. 3. Effects of GTPγS on EPSCs. (**A**) EPSCs were evoked at 0.1 Hz by I_{pCa}. GTPγS (200 μM) was infused into the calyx. Sample recordings before and after GTPγS infusion (a and b) are superimposed. (**B**) Irreversible depression of EPSCs after 10-Hz stimulation (arrows) with GTPγS (0.2 mM) in the presynaptic pipette. Recordings were initiated 20 min after rupture. I_{pCa} did not change throughout the duration of the experiment (upper panel). Sample traces in the middle panel are averaged EPSCs before (1), after the first (2), and after the second (3) 10-Hz train.

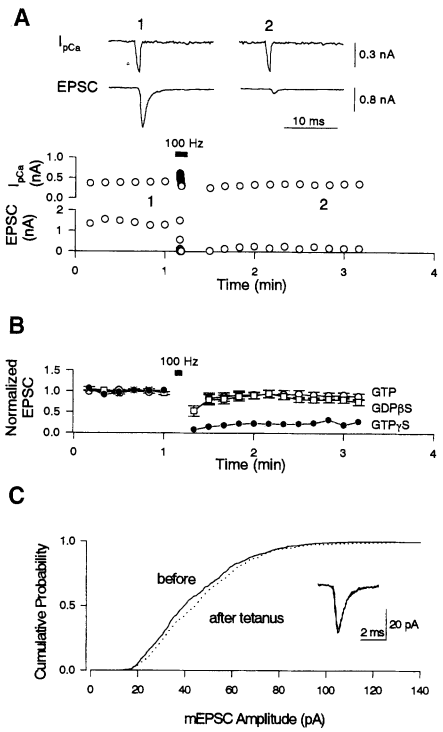

Fig. 4. EPSCs did not recover after a tetanic stimulation with presynaptic GTPγS. (**A**) EPSCs were evoked by I_{pCa} at 0.1 Hz, and a 100-Hz train (10 s) was applied (filled bar). Sample recordings of I_{pCa} and EPSCs before (1) and after (2) the tetanic stimulation are shown above the panel. (**B**) Summarized data for EPSCs at calyces loaded with GTP (0.5 mM, n = 6) (○), GDPβS (3 mM, n = 10) (□), or GTPγS (0.2 mM, n = 6) (●). The amplitude of EPSCs was normalized to that of the control before tetanic stimulation. (**C**) Cumulative amplitude histograms of mEPSCs before (continuous line) and after (dashed line) tetanic stimulation. Data are from a neuron in (A). No significant difference was seen in the Kolmogorov-Smirnov test. (Inset) Sample traces of averaged mEPSCs (each from 20 events) before and after tetanic stimulation (superimposed). The mean amplitude of mEPSCs before and after tetanic stimulation was 29.4 ± 4.2 pA and 30.9 ± 4.3 pA, respectively (n = 6 for each).

References and Notes

1. B. Katz, *The Release of Neural Transmitter Substances* (Liverpool Univ. Press, Liverpool, UK, 1969).
2. J. E. Heuser and T. S. Reese, *J. Cell Biol.* **57**, 315 (1973); W. J. Betz and G. S. Bewick, *Science* **255**, 200 (1992); C. F. Stevens and T. Tsujimoto, *Proc. Natl. Acad. Sci. U.S.A.* **92**, 846 (1995); C. Rosenmund and C. F. Stevens, *Neuron* **16**, 1197 (1996).
3. C. Nuoffer and W. E. Balch, *Annu. Rev. Biochem.* **63**, 949 (1994); S. Ferro-Novic and P. Novic, *Annu. Rev. Cell Biol.* **9**, 575 (1993).
4. S. D. Hess, P. A. Doroshenko, G. J. Augustine, *Science* **259**, 1169 (1993).
5. M. E. Burns, T. Sasaki, Y. Takai, G. J. Augustine, *J. Gen. Physiol.* **111**, 243 (1998).
6. G. J. Augustine *et al.*, *J. Physiol.* **520**, 33 (1999).
7. R. W. Holz, W. H. Brondyk, R. A. Senter, L. Kuizon, I. G. Macara, *J. Biol. Chem.* **269**, 10229 (1994); H. Oishi *et al.*, *J. Biol. Chem.* **273**, 34580 (1998); M. Geppert, Y. Goda, C. F. Stevens, T. C. Sudhof, *Nature* **387**, 810 (1997).
8. I. D. Forsythe, *J. Physiol.* **479**, 381 (1994).
9. T. Takahashi, Y. Kajikawa, T. Tsujimoto, *J. Neurosci.* **18**, 3138. (1998).
10. T. Hori, Y. Takai, T. Takahashi, *J. Neurosci.* **19**, 7262 (1999).
11. Transverse slices (150 μm thick) of superior olivary complex were prepared from 14- to 17-day-old Wistar rats killed by decapitation under halothane anesthesia (*9*, *10*). Using a 60× water immersion objective in an upright microscope, we viewed the calyx of Held and its target, the MNTB principal neuron, with a charge-coupled device camera. The standard artificial cerebrospinal fluid (aCSF) contained (in mM) 120 NaCl, 2.5 KCl, 26 $NaHCO_3$, 1.25 NaH_2PO_4, 2 $CaCl_2$, 1 $MgCl_2$, 10 glucose, 3 myo-inositol, 2 sodium pyruvate, 0.5 ascorbic acid, 4 lactic acid (pH 7.3, gassed with 5% CO_2 and 95% O_2). Bicuculline (10 μM) and strychnine (0.5 μM) were routinely included in the aCSF. The postsynaptic patch pipette contained (in mM) 110 CsF, 30 CsCl, 10 Hepes, 5

EGTA, and 1 $MgCl_2$ (pH 7.3). The standard presynaptic pipette solution contained (in mM) 97.5, potassium gluconate, 32.5 KCl, 10 Hepes, 0.5 EGTA, 1 $MgCl_2$, 10 potassium glutamate, 2.0 Mg-ATP, 12 phosphocreatinine, and 0.5 GTP (pH 7.3). Whole-cell patch-clamp recordings were made from the calyx of Held and MNTB principal neurons, and EPSCs were evoked either by presynaptic action potentials or I_{pCa} elicited by a depolarizing pulse (1-ms duration) (*9*, *10*). For recording presynaptic Ca^{2+} currents, tetraethylammonium chloride (TEA-Cl, 10 mM) and tetrodotoxin (TTX, 1 μM) were added to the aCSF, and potassium gluconate and KCl in the presynaptic pipette solution were replaced by 110 mM CsCl, Hepes was increased to 40 mM, and 10 mM TEA-Cl was added (pH 7.3). The electrode resistance was typically 2 to 4 megohm for the postsynaptic pipette and 5 to 9 megohm for the presynaptic pipette. When EPSCs were evoked by I_{pCa}, the magnitude of the depolarizing pulse was adjusted to about 70% of the maximal size to avoid saturation in the amplitude of the EPSC against I_{pCa}. For recording I_{pCa}, the series resistance (10 to 20 megohm) was compensated by 70 to 80%. Recordings were low-pass filtered at 2.5 to 20 kHz and digitized at 5 to 48 kHz with CED 1401 interface (Cambridge Electronics Design). Leak currents were subtracted for presynaptic Ca^{2+} currents by a P/N protocol (*9*). Recordings were made at room temperature (22° to 26°C). The difference between groups was evaluated by unpaired *t* test or Kolmogorov-Smirnov test, with $P < 0.05$ taken as the level of significance. When GDPβS or GTPγS (both Li^+ salts) was included in the pipette solution, GTP was omitted. Infusion of GDPβS or GTPγS into the calyx was done as previously reported (*10*). Briefly, an Eppendorf yellow tip was heated and pulled to produce a tip diameter of 50 to 70 μm, and the pipette solution containing guanine nucleotides was back-filled into the tube and installed into a patch pipette with its tip positioned by 500 to 600 μm proximal to the tip of the patch pipette. After control responses were recorded, GDPβS or GTPγS was delivered into the patch pipette by a positive pressure manually applied through a syringe. When Lucifer Yellow (0.05%) was injected into a calyx by this method, fluorescence became detectable within 1 min after injection and reached maximal intensity within an additional 2 min. A GDPβS concentration of <0.2 mM in the whole-cell pipette did not prevent the baclofen effect (*9*).

12. The $GABA_B$ receptor ligand baclofen (10 to 20 μM) inhibited EPSCs through activating presynaptic heterotrimeric G proteins (*9*) by 72 ± 4.3% before the presynaptic infusion of GDPβS, but by only 11 ± 2.6% after GDPβS infusion ($n = 4$ cells).
13. I_{pCa} was slightly facilitated during 10-Hz stimulation (*20*, *28*).
14. T. Otis, S. Zhang, L. O. Trussell, *J. Neurosci.* **16**, 7496 (1996).
15. H. von Gersdorff, R. Schneggenburger, S. Weis, E. Neher, *J. Neurosci.* **17**, 8137 (1997).
16. R. Schneggenburger, A. C. Meyer, E. Neher, *Neuron* **23**, 399 (1999).
17. S.-F. Hsu, G. J. Augustine, M. B. Jackson, *Neuron* **17**, 501 (1996); L.-G. Wu and J. G. G. Borst, *Neuron* **23**, 821 (1999).
18. In some experiments GTPγS was photo-released by an ultraviolet flashlight (10 s) from a caged compound included in the presynaptic pipettes (38 μM) (*9*).
19. Recovery was complete with GTP (101 ± 2%, $n = 6$), GDPβS (98 ± 3%, $n = 6$), or with no guanine nucleotides (97 ± 2%, $n = 9$) in the presynaptic pipettes.
20. I. D. Forsythe, T. Tsujimoto, M. Barnes-Davies, M. F. Cuttle, T. Takahashi, *Neuron* **20**, 797 (1998).
21. For comparison, we loaded ATPγS (0.2 mM) into the calyx. Soon after the patch membrane was ruptured, EPSCs started to diminish concomitantly with I_{pCa} and both eventually disappeared within 16 min ($n = 3$). Thus, ATP turnover seems to be indispensable for basal synaptic transmission.
22. J. S. Dittman and W. G. Regehr, *J. Neurosci.* **18**, 6147 (1998); C. F. Stevens and J. F. Wesseling, *Neuron* **21**, 415 (1998); L.-Y. Wang and L. K. Kaczmarek, *Nature* **394**, 384 (1998).
23. A. T. Harootunian *et al.*, *Cell Calcium* **12**, 153 (1991); C. B. Neylon, A. Nickashin, V. A. Tkachuk, A. Bobik, *Cell Calcium* **23**, 281 (1998).
24. T. Takahashi and T. Ishikawa, unpublished observation.
25. M. Rupnik, G. J. Law, A. J. Northrop, W. T. Mason, R. Zorec, *Neuroreport* **6**, 853 (1995); M.-C. Galas *et al.*, *J. Biol. Chem.* **272**, 2788 (1997); U. Ashery, H. Koch, V. Scheuss, N. Brose, J. Rettig, *Proc. Natl. Acad. Sci. U.S.A.* **96**, 1094 (1999).
26. M. Nagao, Y. Kajiro, H. Itoh, *Oncogene* **18**, 4425 (1999).
27. J. E. Hinshaw and S. L. Schmidt, *Nature* **374**, 190 (1995); K. Takei *et al.*, *Nature* **374**, 186 (1995).
28. M. F. Cuttle, T. Tsujimoto, I. D. Forsythe, T. Takahashi, *J. Physiol.* **512**, 723. (1998).
29. We thank H. Kasai, T. Manabe, B. Robertson, D. Saffen, A. Silver, M. Tachibana, and Y. Takai for discussions and comments. Supported by the Research for the Future Program of the Japan Society for the Promotion of Sciences.

11 January 2000; accepted 23 May 2000

Abolition and Reversal of Strain Differences in Behavioral Responses to Drugs of Abuse After a Brief Experience

Simona Cabib,[1] Cristina Orsini,[1] Michel Le Moal,[2] Pier Vincenzo Piazza[2]*

Inbred strains of mice are largely used to identify the genetic basis of normal and pathological behaviors. This report demonstrates that a moderate period of food shortage, an ecologically common experience, can reverse or abolish strain differences in behavioral responses to the abused psychostimulant amphetamine. The period of food shortage occurred when the animals were mature and was terminated before the administration of amphetamine. Strain differences in behavior appear highly dependent on environmental experiences. Consequently, to identify biological determinants of behavior, an integrated approach considering the interaction between environmental and genetic factors needs to be used.

Genetic analyses using inbred strains of mice are increasingly utilized to identify biological determinants of normal and pathological behaviors (*1*–*3*). A basic prerequisite of these investigations is the existence of consistent and reliable behavioral differences between inbred strains, which are then used to identify the genetic determinant of behavioral phenotypes (*1*, *2*, *4*). A recent report described variation in the behavior of inbred strains that can occur across laboratories (*4*). These results are particularly troubling because they are observed despite the explicit effort to maintain identical experimental settings and environmental conditions. Although the authors restrict the effects of environmental variables to phenotypes with a small genetic influence, doubt remains as to whether major gene-environment interactions might be currently overlooked.

We studied the effects of food shortage on strain differences in behavioral phenotypes related to drug abuse, a behavioral pathology considered to have strong genetic influences (*5*). Food shortage was chosen for three reasons. First, it is a common and ecologically relevant environmental experience very likely to occur during the life-span of animals living in the wild. Second, it is often used in laboratory settings because it accompanies learning tests based on positive reinforcers including drugs of abuse (*6*). Third, food shortage increases the activity of biological systems mediating behavioral responses to drugs of abuse, such as the mesencephalic dopaminergic transmission and glucocorticoid secretion (*7*). Mice from the C57BL/6JIco and DBA/2JIco inbred strains were studied (*8*). C57BL/6J and DBA/2J are among the oldest and most studied inbred strains (*3*), and the recombinant inbred strains derived from them are largely used for quantitative trait loci (QTL) analysis (*1*). Two behaviors induced by the abused psychostimulant amphetamine were studied: locomotion and place conditioning. Drug-induced locomotion is the test most often used for evaluating the motor-stimulating effect of psychostimulant drugs (*9*). It represents a simple unconditioned response where genetic influences have been well characterized (*4*, *10*). In place conditioning, aversive or rewarding effects of drugs are inferred from measuring, in a drug-free state, preference

[1]Dipartimento di Psicologia, Università "La Sapienza" via dei Marsi 78, Roma I-00185, Italy. [2]Laboratoire de Psychobiologie des Comportement Adaptatifs, INSERM Unit 259, Institute François Magendie, University of Bordeaux II, Rue Camille St. Saens, Domaine de Carreire, Bordeaux Cedex, France.

*To whom correspondence should be addressed. E-mail: pier-vincenzo.piazza@bordeaux.inserm.fr